AIP Advances

# High performance and transparent multilayer MoS2 transistors: Tuning Schottky barrier characteristics

Young Ki Hong, Geonwook Yoo, Junyeon Kwon, Seongin Hong, Won Geun Song, Na Liu, Inturu Omkaram, Byungwook Yoo, Sanghyun Ju, Sunkook Kim, and Min Suk Oh

Citation: AIP Advances **6**, 055026 (2016); doi: 10.1063/1.4953062
View online: http://dx.doi.org/10.1063/1.4953062
View Table of Contents: http://scitation.aip.org/content/aip/journal/adva/6/5?ver=pdfcov
Published by the AIP Publishing



# High performance and transparent multilayer $MoS_2$ transistors: Tuning Schottky barrier characteristics

Young Ki Hong,[1,a] Geonwook Yoo,[2,a] Junyeon Kwon,[1] Seongin Hong,[1] Won Geun Song,[1] Na Liu,[1] Inturu Omkaram,[1] Byungwook Yoo,[2] Sanghyun Ju,[3] Sunkook Kim,[1,b] and Min Suk Oh[2,b]

[1]*Multi-Functional Bio/Nano Lab., Kyung Hee University, Gyeonggi 446-701, South Korea*
[2]*Display Convergence Research Center, Korea Electronics Technology Institute, Gyeonggi 463-816, South Korea*
[3]*Department of Physics, Kyonggi University, Suwon, Gyeonggi-Do 443-760, South Korea*

(Received 29 December 2015; accepted 18 May 2016; published online 25 May 2016)

Various strategies and mechanisms have been suggested for investigating a Schottky contact behavior in molybdenum disulfide ($MoS_2$) thin-film transistor (TFT), which are still in much debate and controversy. As one of promising breakthrough for transparent electronics with a high device performance, we have realized $MoS_2$ TFTs with source/drain electrodes consisting of transparent bi-layers of a conducting oxide over a thin film of low work function metal. Intercalation of a low work function metal layer, such as aluminum, between $MoS_2$ and transparent source/drain electrodes makes it possible to optimize the Schottky contact characteristics, resulting in about 24-fold and 3 orders of magnitude enhancement of the field-effect mobility and on-off current ratio, respectively, as well as transmittance of 87.4 % in the visible wavelength range.  [http://dx.doi.org/10.1063/1.4953062]

Recently, two-dimensional (2-D) layered transition metal dichalcogenides such as molybdenum disulfide ($MoS_2$) have drawn great interests as a promising channel material of thin-film transistors (TFTs) for high-performance transparent and flexible electronics.[1–7] $MoS_2$ has a relatively large direct or indirect band gap (1.2–1.8 eV) depending on a number of layers,[8] a high mobility (~200 $cm^2/Vs$) with a high-$k$ dielectric layer,[9] and absence of dangling bonds.[10] Moreover, its atomically thin 2-D layered structure is suitable for TFT architectures, and therefore $MoS_2$ can have an advantage of relatively simple fabrication process steps for large-area and low-cost electronics. These unique properties have been facilitating substantial research efforts to understand electrical and optical properties,[8–11] to find proper transparent contact electrodes,[2,3,12] and to propose various device structures,[13] which are important to design TFTs for emerging display applications.

Especially, transparent contact electrodes to $MoS_2$ have been investigated in various approaches since they are one of the major performance limiting factors. Conventional transparent conducting oxides (TCOs), such as indium tin oxide (ITO) or indium zinc oxide (IZO), have a high work-function of ~5 eV, and therefore result in a large Schottky barrier height (SBH, $\Phi_B$) at the $MoS_2$ contact area due to Fermi-level pinning effect. To improve the interfacial characteristics between IZO source/drain (S/D) electrodes and multilayer $MoS_2$, and thus to realize a high performance $MoS_2$ TFT, a selective laser annealing technique with high energy density and a short wavelength was demonstrated by Kwon *et al.*[14] Still, a Schottky contact instead of an Ohmic contact at most S/D electrodes-$MoS_2$ interfaces is inevitable because of its relatively large bandgap and lack of controllable as well as stable doping methods. On the other hand, recent studies reported that hetero-contacts and/or -structures with graphene electrodes could provide a high performance

[a]Y. K. Hong and G. Yoo contributed equally to this work.
[b]Electronic mail: kimskcnt@gmail.com, ohms@keti.re.kr

 

transparent contact to $MoS_2$ channel layer since the graphene had same hexagonal structure with no dangling bonds and their unique 2-D to 2-D interface could lead to a small SBH.[15,16] However, the reported electrical properties, specifically field-effect mobility, are not good enough as driving TFT switches and circuitry for future displays. Furthermore, the expensive laser annealing technique is not practical for large-area fabrication.

In this report, we demonstrate a high-performance transparent $MoS_2$ TFT with bi-layered S/D electrodes consisting of aluminum (Al) and IZO without post-annealing process. Thin Al layers have been used as a transparent metal electrode in OLEDs and other light emitting structures due to its good optical transparency with decreasing thickness. Here, Al-IZO (10 and 100 nm, respectively) S/D electrodes show transmittance of 87.4 % in the visible range (380–750 nm). The low work-function (4.06–4.26 eV) of Al contributes to lowering a SBH, resulting in a reduction in contact resistance. Our transparent $MoS_2$ TFTs exhibits significant enhancement of the device performances, for examples, about 24-fold and 3 orders of magnitude increases of the field-effect mobility ($\mu_{eff}$) and on-off current ratio ($I_{on}/I_{off}$), respectively.

Figure 1(a) shows a 3-D schematic illustration of the transparent multilayer $MoS_2$ TFT with back-gate and bi-layered S/D electrodes. Among the various TCOs, ITO-Glass (ITO thickness = 200 nm) was selected for transparent back-gate electrode as well as substrate. For a high $k$ gate insulator (GI), an amorphous aluminum oxide ($Al_2O_3$) with a thickness of 40 nm was deposited on the ITO-Glass by atomic layer deposition (ALD, Lucida D100, South Korea) process using trimethylaluminum as an Al precursor and $H_2O$ as an oxidant, respectively. Multilayer $MoS_2$ used as active channel was mechanically exfoliated from bulk crystal (supplied from SPI, USA) and

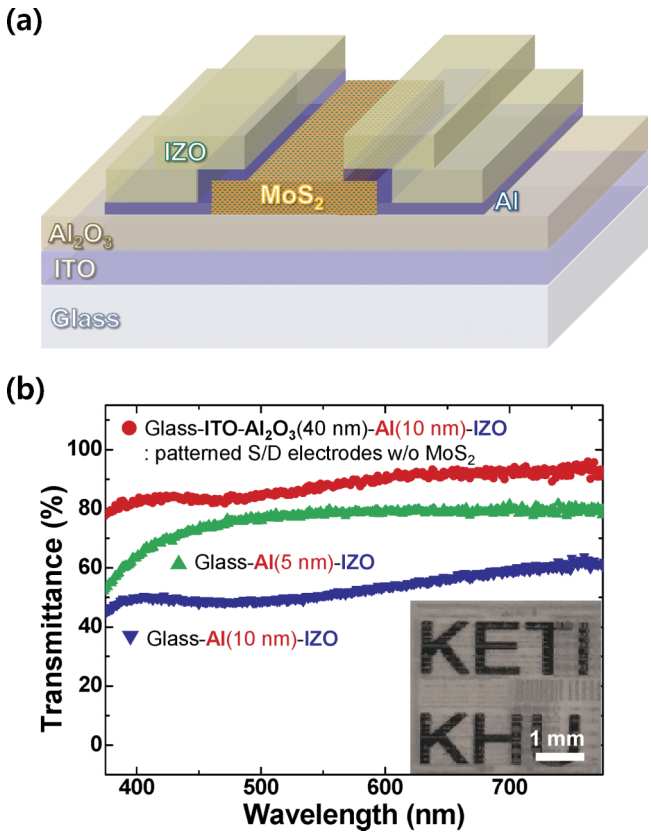


FIG. 1. (a) 3D schematic illustration of the transparent $MoS_2$ TFT. Thin Al layer was intercalated at contact regions between IZO S/D electrodes and multilayered $MoS_2$ channel. (b) Transmission spectra of the TFT configuration using patterned Al-IZO (●: $t_{Al} = 10$ nm) including ITO-$Al_2O_3$ layers and continuous bi-layers of Al-IZO with different Al thicknesses (▲: $t_{Al} = 5$ nm and ▼: $t_{Al} = 10$ nm) in the visible wavelength range. The thickness of all the IZO layer was fixed at 100 nm. Inset: Photograph of the TFT patterned Al-IZO bi-layer on the printed texts.

transferred onto the GI through the well-known scotch-tape method.[11,17] Thin Al layers with various thicknesses (5, 10, and 20 nm) were deposited by thermal evaporator. Then, a 100-nm-thick IZO was fabricated using RF magnetron sputtering. A molar ratio of $In_2O_3$ to ZnO was controlled to 1 : 1, and the corresponding IZO exhibited a work function of 4.67 eV.[18,19] Finally, Al-IZO bi-layered structure of S/D electrodes was simultaneously patterned into TFT configurations through photolithography and wet etching process. For a control experiment, we also fabricated a transparent $MoS_2$ TFT without Al layer. It should be noted that post thermal annealing or laser irradiation were not applied to both transparent TFTs. The Al layer, which was intercalated at the contact region of S/D electrodes and active channel, provides modulation of SB characteristics between IZO and $MoS_2$ and it will be discussed in details at the following section.

Figure 1(b) compares transmission spectra (JASCO V-560) of Al-IZO layers in terms of the Al thicknesses as well as layer-configurations, in which the thickness of all the IZO was fixed at 100 nm. As increasing the thickness of the Al layer from 5 nm to 10 nm, transmission spectra of corresponding Al-IZO layers with continuous (*i.e.*, non-patterned) configuration were clearly reduced over entire wavelength range. The average transmittances of Al-IZO layers with the Al thicknesses of 5, 10, and 20 nm were evaluated as 75.7 %, 52.3 %, and 17.7 %, respectively (spectrum for the 20-nm-thick Al-IZO not shown here). In order to investigate the effect of Al intercalating layer on transparency of actual TFTs array, we fabricated Al(10 nm)-IZO layer with discontinuous (*e.g.*, patterned) configuration onto the ITO(200 nm)-$Al_2O_3$ (40 nm) substrate, which showed distinct enhancement of transmittance in overall wavelength range, even comparing with that of 5-nm-thick Al-IZO, as shown in Fig. 1(b). It should be noted that patterned Al-IZO layer did not contain any $MoS_2$ flake based on the following reasons; (i) active layers of TFTs and/or capacitors in driving circuitry (for example, 6 Tr. & 2 Cap.) occupied very limited space in whole display panel. (ii) Al influenced the transparency of the device more dominantly than multilayer $MoS_2$ flakes. The average transmittance of the patterned Al-IZO on ITO-$Al_2O_3$ substrate was calculated to 87.4 %, which comparably agreed on our previous report by considering that of spray-coated multilayer $MoS_2$ flakes.[12,20] As shown in the inset of Fig. 1(b), the printed texts were clearly recognized through the TFT patterns of the Al-IZO including ITO and $Al_2O_3$ layers.

Figure 2 presents the electrical properties of our transparent multilayer $MoS_2$ TFTs with and without the Al intercalating layer. As shown in the transfer characteristic curves ($I_{ds}$-$V_{gs}$) at $V_{ds}$ = 1 V (Fig. 2(a)), both devices show *n*-type behaviors.[12,21–23] For Al-intercalated TFT, current level in on-state and subthreshold swing were clearly improved, and $I_{on}/I_{off}$ was increased from $10^4$ to $10^7$. Field-effect mobility ($\mu_{eff}$), one of key factors to evaluate TFT performance, can be calculated as;

$$\mu_{eff} = \frac{L}{WC_{GI}V_{ds}} \frac{dI_{ds}}{dV_{gs}}\bigg|_{V_{ds}=1V}$$

where $L$, $W$, and $C_{GI}$ denote channel length, channel width, and GI capacitance, respectively. The $\mu_{eff}$ of the transparent $MoS_2$ TFT ($W/L$ = 1.8/3.6 μm) without Al layer was calculated to be 1.4 $cm^2$/Vs, which was well-agreed with our previous report.[12] It has been reported that conductivity of IZO lies within 2,000−3,000 S/cm depending on its atomic composition ratio,[18] which is about 2 orders of magnitude lower than conventional metal. So, poor device performance of the transparent TFT with only IZO S/D electrodes could be attributed to large SBH and relatively lower conductivity. By introducing Al intercalation, the $\mu_{eff}$ of the device with $W/L$ of 10.5/9.6 μm was dramatically enhanced up to 24 folds as 33.6 $cm^2$/Vs. Figure 2(b) shows output characteristic curves ($I_{ds}$-$V_{ds}$) of the Al-intercalated transparent TFT. Robust current saturation in the large $V_{ds}$ region was identified, implying our device as an attractive candidate for various transparent sensor and/or display applications. Magnifications of the $I_{ds}$-$V_{ds}$ curves in the small $V_{ds}$ region are presented in Figs. 2(c) and 2(d), respectively. The higher current levels as well as the better linear relationship of Fig. 2(c), as compared to Fig. 2(d), revealed that Schottky contacts between $MoS_2$ active channel and bi-layered Al-IZO S/D electrodes were clearly improved, which could also attribute to the elevated performances of our transparent TFTs. It should be noted that there existed a thin layer of native $Al_2O_3$ on the top of Al layer, because it was exposed to atmospheric environments before IZO sputtering procedure. This amorphous $Al_2O_3$ layer might act as charge tunneling barrier between

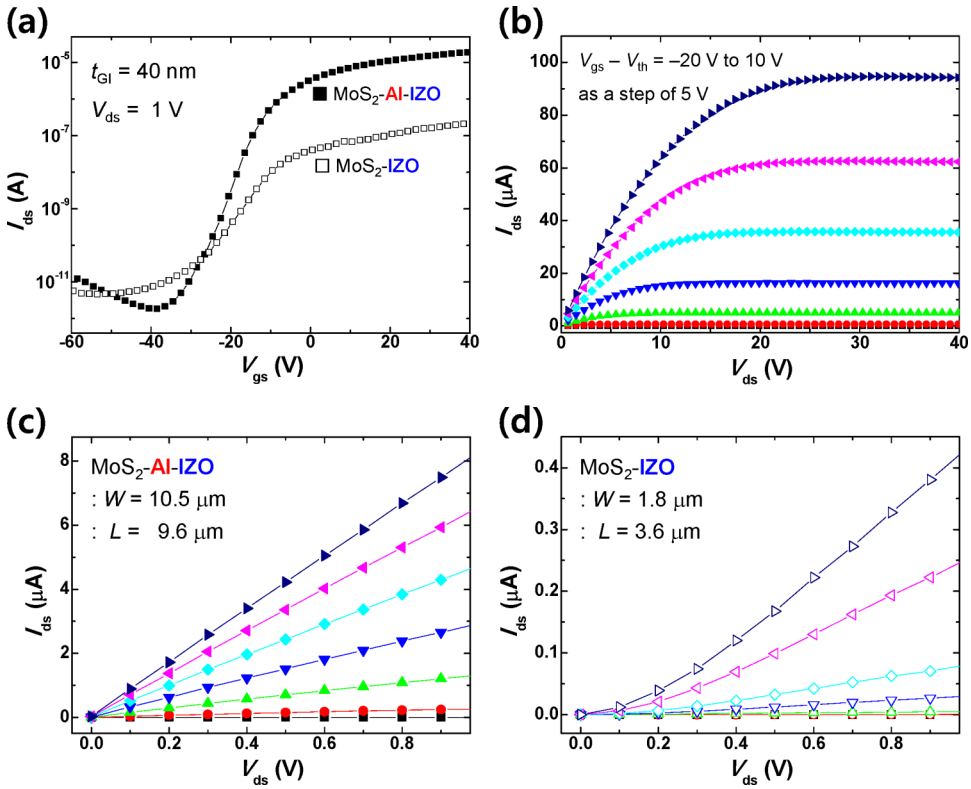


FIG. 2. (a) Transfer characteristic of the transparent $MoS_2$ TFT at $V_{ds}$ = 1 V without (■) and with (□) Al layer. (b) Output characteristic curves of the transparent $MoS_2$ TFT with Al intercalating layer. $V_{gs} - -V_{th}$ were applied from −20 to 10 V as a step of 5 V. Magnification of the output characteristics of the semi-trasparent TFT in the small $V_{ds}$ region; (c) with and (d) without Al intercalating layer.

Al and IZO, which would influence the TFT performances detrimentally. However, this undesirable $Al_2O_3$ layer can be minimized by refining fabrication procedure, for example, sequential deposition of bi-layered S/D electrode without breaking vacuum.

The nature of $MoS_2$-metal contact is still in much debate with controversial experimental results, which would be Ohmic or Schottky as well as *n*- or *p*-type.[10,21,24,25] After the systematic investigation of $MoS_2$-metal contact with respect to various work function from scandium (3.5 eV) to platinum (5.9 eV), reported by Das *et al.*,[21] diverse approaches have been made to control and understand the contact behaviors in $MoS_2$-metal junction. For examples, Kawakami and co-workers reported that the insertion of thin magnesium oxide as tunneling barrier between ferromagnetic cobalt electrodes and single layer $MoS_2$ resulted in more efficient spin injection and transport due to the lowering of the SBH.[26] Also, SBH and width in single layer $MoS_2$ TFT were quantitatively controlled by varying contact area of titanium-gold S/D electrodes.[27] Recently, SB and charge injection/transport characteristics of 2-D layered materials were studied with respect to interface geometry at semiconductor-metal junction, such as top-contact vs. edge-contact.[28,29]

Considering those reports in the related research fields, our strategy using thin metal layer with low work function and conventional top-contact configuration could offer solid advantages toward the transparent opto-electronic applications. As shown in Fig. 3, energy band diagrams of $MoS_2$-IZO and $MoS_2$-Al-IZO contacts provide an intuitive comprehension about the effect of the Al intercalating layer on the SB in our transparent $MoS_2$ TFT. By using atomic force microscopy (XE7 AFM, Park Systems, South Korea), the thicknesses of the multilayer $MoS_2$ flakes were estimated to be 30.0 ± 1.8 nm for the transparent TFT without Al layer and 39.0 ± 7.4 nm for the Al intercalated one, respectively, implying energy band gap ($E_g$) of 1.2 eV. In addition, multilayer $MoS_2$ for transparent TFT with Al layer has rougher surface than that without Al, which would indicate that the lowering of the SBH due to the Al layer functioned properly even in harsh interfacial environment.

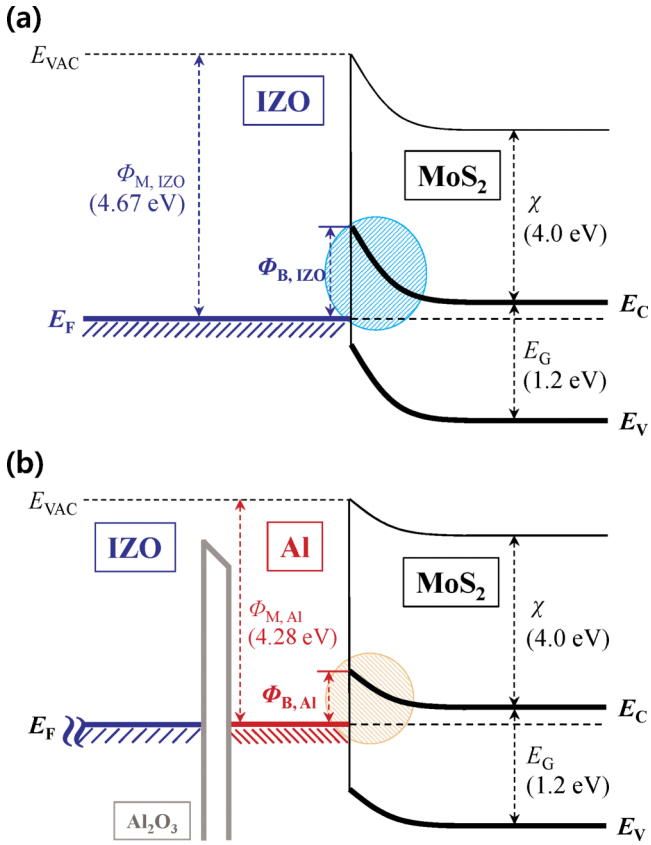


FIG. 3. Energy band diagrams between S/D electrodes and active channel; (a) $MoS_2$-IZO contact and (b) $MoS_2$-Al-IZO contact including thin layer of amorphous $Al_2O_3$. SB in each case was depicted by corresponding color-dashed area.

In conclusion, we have successfully fabricated a high-performance and transparent $MoS_2$ TFT based on Al-IZO bi-layered S/D electrodes, which showed averaged transmittance of 87.4% in the visible region, $\mu_{eff}$ of 33.6 $cm^2/Vs$, and $I_{on}/I_{off}$ of $10^7$. The Al layer with optimized thickness has guaranteed the outstanding device performances, which could be attributed to the sufficient lowering of the SBH. Furthermore, it is highly expected that device performances of our transparent TFT with bi-layered S/D electrodes can be improved by applying post-engineering for reducing carrier scattering through high $k$-dielectric encapsulation[30] or charge transfer doping[31] as well as conventional strategies for reducing contact resistance, such as thermal[11,17] or laser[12,14] annealing. Our high-performance transparent 2D layered transistors with bi-layered S/D electrodes provide the state-of-art in a high resolution and transparent display.

## ACKNOWLEDGEMENT

This work was supported by the Industrial Strategic Technology Development Program under Grant 10045145, and was also supported by the National Research Foundation of Korea (NRF-2013M3C1A3059590 and 2014R1A2A1A11049450)

[1] H. Y. Chang, S. Yang, J. Lee, L. Tao, W. S. Hwang, D. Jena, N. Lu, and D. Akinwande, ACS Nano **7**, 5446 (2013).
[2] G. H. Lee, Y. J. Yu, X. Cui, N. Petrone, C. H. Lee, M. S. Choi, D. Y. Lee, C. Lee, W. J. Yoo, K. Watanabe, T. Taniguchi, C. Nuckolls, P. Kim, and J. Hone, ACS Nano **7**, 7931 (2013).
[3] J. Yoon, W. Park, G. Y. Bae, Y. Kim, H. S. Jang, Y. Hyun, S. K. Lim, Y. H. Kahng, W. K. Hong, B. H. Lee, and H. C. Ko, Small **9**, 3295 (2013).
[4] R. Cheng, S. Jiang, Y. Chen, Y. Liu, N. Weiss, H. C. Cheng, H. Wu, Y. Huang, and X. Duan, Nat. Commun. **5**, 5143 (2014).
[5] J. Pu, L. J. Li, and T. Takenobu, Phys. Chem. Chem. Phys. **16**, 14996 (2014).
[6] D. Akinwande, N. Petrone, and J. Hone, Nat. Commun. **5**, 5678 (2015).

[7] W. Zhu, M. N. Yogeesh, S. Yang, S. H. Aldave, J. S. Kim, S. Sonde, L. Tao, N. Lu, and D. Akinwande, Nano Lett. **15**, 1883 (2015).
[8] K. F. Mak, C. Lee, J. Hone, J. Shan, and T. F. Heinz, Phys Rev Lett **105**, 136805 (2010).
[9] L. Liu, S. B. Kumar, Y. Ouyang, and J. Guo, IEEE Trans. Electron Devices **58**, 3042 (2011).
[10] B. Radisavljevic, A. Radenovic, J. Brivio, V. Giacometti, and A. Kis, Nat. Nanotechnol. **6**, 147 (2011).
[11] W. Choi, M. Y. Cho, A. Konar, J. H. Lee, G. B. Cha, S. C. Hong, S. Kim, J. Kim, D. Jena, J. Joo, and S. Kim, Adv. Mater. **24**, 5832 (2012).
[12] J. Kwon, Y. K. Hong, H. J. Kwon, Y. J. Park, B. Yoo, J. Kim, C. P. Grigoropoulos, M. S. Oh, and S. Kim, Nanotechnology **26**, 035202 (2015).
[13] X. Zou, J. Wang, C.-H. Chiu, Y. Wu, X. Xiao, C. Jiang, W.-W. Wu, L. Mai, T. Chen, J. Li, J. C. Ho, and L. Liao, Adv. Mater. **26**, 6255 (2014).
[14] H. Kwon, W. Choi, D. Lee, Y. Lee, J. Kwon, B. Yoo, C. P. Grigoropoulos, and S. Kim, Nano Res. **7**, 1137 (2014).
[15] Y. Du, L. Yang, J. Zhang, H. Liu, K. Majumdar, P. D. Kirsch, and P. D. Ye, IEEE Electron Device Lett. **35**, 599 (2014).
[16] A. Di Bartolomeo, Phys. Rep. **606**, 1 (2016).
[17] S. Kim, A. Konar, W. S. Hwang, J. H. Lee, J. Lee, J. Yang, C. Jung, H. Kim, J. B. Yoo, J. Y. Choi, Y. W. Jin, S. Y. Lee, D. Jena, W. Choi, and K. Kim, Nat. Commun. **3**, 1011 (2012).
[18] M. P. Taylor, D. W. Readey, M. F. A. M. Van Hest, C. W. Teplin, J. L. Alleman, M. S. Dabney, L. M. Gedvilas, B. M. Keyes, B. To, J. D. Perkins, and D. S. Ginley, Adv. Funct. Mater. **18**, 3169 (2008).
[19] W. L. Leong, Y. Ren, H. L. Seng, Z. Huang, S. Y. Chiam, and A. Dodabalapur, ACS Appl. Mater. Interfaces **7**, 11099 (2015).
[20] B. Lei, G. R. Li, and X. P. Gao, J. Mater. Chem. A **2**, 3919 (2014).
[21] S. Das, H. Y. Chen, A. V. Penumatcha, and J. Appenzeller, Nano Lett. **13**, 100 (2013).
[22] W. Zhou, X. Zou, S. Najmaei, Z. Liu, Y. Shi, J. Kong, J. Lou, P. M. Ajayan, B. I. Yakobson, and J. C. Idrobo, Nano Lett. **13**, 2615 (2013).
[23] S. McDonnell, R. Addou, C. Buie, R. M. Wallace, and C. L. Hinkle, ACS Nano **8**, 2880 (2014).
[24] M. Fontana, T. Deppe, A. K. Boyd, M. Rinzan, A. Y. Liu, M. Paranjape, and P. Barbara, Sci. Rep. **3**, 1634 (2013).
[25] C. Gong, L. Colombo, R. M. Wallace, and K. Cho, Nano Lett. **14**, 1714 (2014).
[26] J. R. Chen, P. M. Odenthal, A. G. Swartz, G. C. Floyd, H. Wen, K. Y. Luo, and R. K. Kawakami, Nano Lett. **13**, 3106 (2013).
[27] H. Liu, M. Si, Y. Deng, A. T. Neal, Y. Du, S. Najmaei, P. M. Ajayan, J. Lou, and P. D. Ye, ACS Nano **8**, 1031 (2014).
[28] L. Wang, I. Meric, P. Y. Huang, Q. Gao, Y. Gao, H. Tran, T. Taniguchi, K. Watanabe, L. M. Campos, D. A. Muller, J. Guo, P. Kim, J. Hone, K. L. Shepard, and C. R. Dean, Science **342**, 614 (2013).
[29] A. Allain, J. Kang, K. Banerjee, and A. Kis, Nat. Mater. **14**, 1195 (2015).
[30] S. L. Li, K. Tsukagoshi, E. Orgiu, and P. Samorì, Chem. Soc. Rev. **45**, 118 (2016).
[31] H. Schmidt, F. Giustiniano, and G. Eda, Chem. Soc. Rev. **44**, 7715 (2015).